UNITED STATES DEPARTMENT OF COMMERCE
National Institute of Standards and Technology
Gaithersburg, Maryland 20899-

July 21, 2016

50-184
TR-5

ATTN: Document Control Desk
U.S. Nuclear Regulatory Commission
Washington, DC 20555-0001

Subject: Response to Request for Additional Information on Preliminary Safety Analysis Report (TAC no. MF7235).

Dear Sirs/Madams:

On April 25, 2016, National Institute of Standards and Technologies Center for Neutron Research (NCNR) received a request for additional information (RAI) concerning the Preliminary Safety Analysis Report in support of conversion of the National Bureau of Standards Reactor (NBSR) to low-enriched uranium fuel. Attached is our response to that request.
Please contact me at (301) 975-6260 if there are any questions.

Sincerely,

Thomas H. Newton, Jr., Ph.D.
Deputy Director
NIST Center for Neutron Research

I certify under penalty of perjury that the following is true and correct.

Enclosures (nos. 2-8 sent electronically):

1- Response to RAIs
2- Report BNL-99145-2013-IR, Brown, Hanson, and Diamond (RAI #2 and #12)
3- Sudo and Kaminaga CHF paper (1993)
4- Kaminaga, Yamamoto, and Sudo technical report on CHF Correlation (1998)
5- Saha and Zuber paper on vapor generation (1974)
6- RELAP5 input
7- HOTSPOT output
8- NBS 1980

Cc: U.S. Nuclear Regulatory Commission
ATTN: Xiaosong Yin
One White Flint North
11555 Rockville Pike, M/S O12D20
Rockville, MD 20852

A020
NRR

NIST

RESPONSES TO

U.S. NUCLEAR REGULATORY COMMISSION

REQUEST FOR ADDITIONAL INFORMATION

REGARDING CONVERSION PRELIMINARY SAFETY ANALYSIS REPORT FOR THE

NATIONAL INSTITUTE OF STANDARDS AND TECHNOLOGY TEST REACTOR (NBSR)

By letter dated December 30, 2014 (Agencywide Documents Access and Management System (ADAMS) Accession No. ML15028A135), the National Institute of Standards and Technology (NIST) Center for Neutron Research submitted a Preliminary Safety Analysis Report (PSAR) for the conversion of the NIST test reactor (aka NBSR) from high-enriched uranium (HEU) to low-enriched uranium (LEU) fuel.

The U.S. Nuclear Regulatory Commission (NRC) is reviewing the PSAR regarding the technical adequacy of the document. After reviewing the PSAR, questions have arisen that require additional information and clarification (ADAMS Accession No. ML16103A140). This document provides the responses to those requests for additional information (RAIs).

RAI No. 1:

The PSAR states that a Monte Carlo Neutron Photon (MCNP) computer model of the NBSR core had been developed, and a version of the MCNP was used as the primary reactor physics modeling tool.

NUREG-1537, Part 1, "Guidelines for Preparing and Reviewing Applications for the Licensing of Non-Power Reactors: Format and Content," Section 4.5, "Nuclear Design," states, in part, that "Computer codes that are used should be described in detail as to the name and type of code, the way it is used, and its validity on the basis of experiments or confirmed predictions of operation non-power reactors."

The PSAR does not indicate such validity and/or comparisons that confirmed predictions have been established to confirm the acceptability of the MCNP model. In addition, in the NIST 2004 version of Safety Analysis Report (SAR), it states, in part, that "The power distribution, excess reactivity, shutdown margin, reactivity coefficients, and core thermal-hydraulic behavior are calculated and compared to measurements." However, such comparisons cannot be found in the SAR. In SAR Tables 4.5.4 and 4.5.2, there are some comparisons of control rods worth and some calculations to indicate critical condition reactivity differences, however, they do not indicate if there are acceptable agreements.

Provide comparisons of calculated and measured parameters for NBSR that demonstrate that the MCNP model utilized is suitable for the prediction of parameters to assess the validity of the use of the MCNP model. At a minimum, this should include estimated critical position, control rod worth, and the isothermal-temperature coefficient for sufficient cases to demonstrate validity.

Any such comparison should also establish the basis for acceptability.

Response to RAI No. 1:

MCNP (Monte Carlo N-Particle) is used for the analysis of the NBSR because it can provide accurate simulations of neutron transport, it is capable of handling the complex geometry of the reactor, and it has been coupled to burnup codes so that the depletion of the fuel and buildup of fission products can also be modeled. Numerous comparisons of MCNP calculations with measurements of various kinds can be found in the literature and show its well-known capability. With respect to research and test reactors, it has been widely used, including for reactors licensed by the NRC. Among other applications at the NBSR, it was used for the safety analysis for the NBSR license renewal submission in 2004. However, to provide full qualification of the use of the code, it should be shown that it can also reproduce measurements made at the NBSR. This is done below using measurements of critical shim arm position and shim arm reactivity worth. A discussion of the isothermal temperature coefficient (ITC) is also included.

Section 4.5.1.1 of the PSAR states that for "the initial and final (fully withdrawn) measured shim arm positions the code gives a multiplication constant (k_{eff}) of unity, within an acceptable uncertainty." At beginning-of-cycle, this is taken care of by adjusting the shim arm position and at end-of-cycle the shim arms are totally removed and k_{eff} is ~1.006, differing from unity by only ~0.6 %Δk/k. These calculations are for an idealized fuel cycle of 38.5 days; in reality the cycle length varies slightly each cycle.

Figure 1 provides another perspective on the calculation of critical shim arm angle taking into account the depletion of material in the shim arms. The three sets of data points on the graph are critical shim arm positions at startup (before xenon buildup) as a function of fuel cycle starting with new replacements of shim arms during the period 1995-2008. Since the shim arms are replaced every few years, there are additional data points for the periods before 1995 and after 2008 that are not shown on the graph. The data vary at startup due to differences in regulating rod position, length of previous cycle, and coolant temperature. The solid curve is the corresponding calculation assuming that all cycles are identical. As stated in Section 4.5.2.1 of the PSAR, shim arms are now replaced after 25 cycles.

For this limited set of data, the calculation is approximately 0.5 degree below the average of the data and this corresponds to a small bias of ~0.45 %Δk/k. The latter is based on using a shim arm worth of 0.9 %Δk/k/degree (cf discussion of shim arm differential worth that follows) at a critical shim arm position of 22°.

The agreement between calculated and measured total shim arm worth is another gauge of how good the MCNP model is. Table 4.6 in Section 4.5.2.1 gives the calculated worths for fresh shim arms. However, in Section 4.5.1.1 incorrect units ($ rather than %Δk/k) are given for the same calculations. The units of the measured values at startup given in the same section are correct. Converting the measured values to the same units as the calculated values gives a measurement of 25.2±2.5 %Δk/k averaged over many cycles. The calculations give a worth of 24.9 %Δk/k for fresh shim arms diminishing by 22% (cf Section 4.5.2.1) to a worth of 19.4 %Δk/k at the end of their life. This is considered sufficiently accurate and is in the direction so as to make the calculations of shim arm worth conservative (i.e., lower than the measured value).

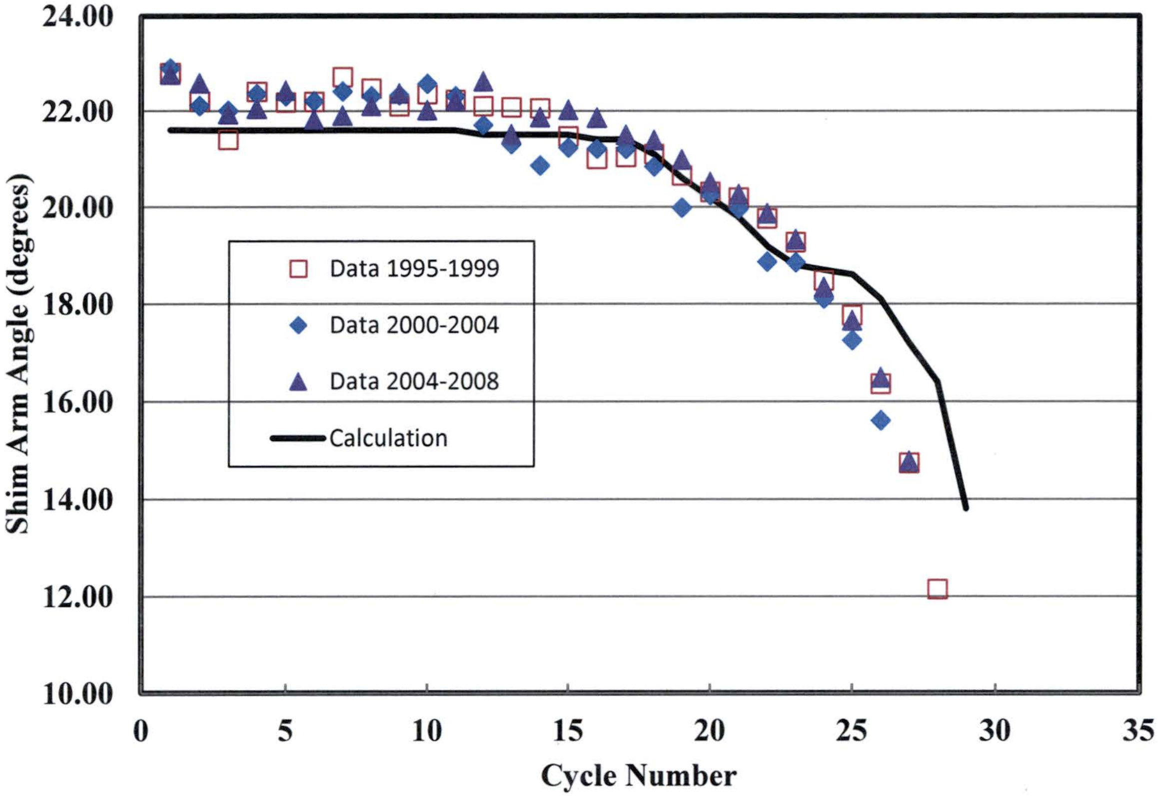

Figure 1-1 Shim arm critical angle as a function of cycle

The shim arm worth as a function of shim arm angle at startup is given in Figure 1-2 below based on measurements made for the last set of new shim arms in 2013. The measured data are obtained for each shim arm (with the remaining three shim arms positioned to maintain criticality for each position) and show the variation due to the different location of each arm. The corresponding calculation is for an average of the individual shim arms moved through one-degree steps. The agreement is considered good.

The isothermal temperature coefficient is not routinely measured; however, a measurement was made as part of the initial testing of the NBSR[a] in 1969 when the core was filled with fuel elements containing 170 gm of ^{235}U rather than 350 gm as presently used. The measured value at that time was –(0.023-0.035) %Δk/k/°C over a temperature range of 23-49°C. The calculated value for the current HEU core, given in Table 4.10 of the PSAR (correcting for an error in addition in the table) is -0.031 %Δk/k/°C. This value was calculated using temperature changes of 20-77°C for the scattering kernel and 46-96°C for the density changes. Although the two cannot be easily quantitatively compared because they are for two different cores and different temperature ranges, they do show qualitative agreement.

[a] "Report on the Initial Startup and Testing of the NBSR," National Bureau of Standards, September 1969.

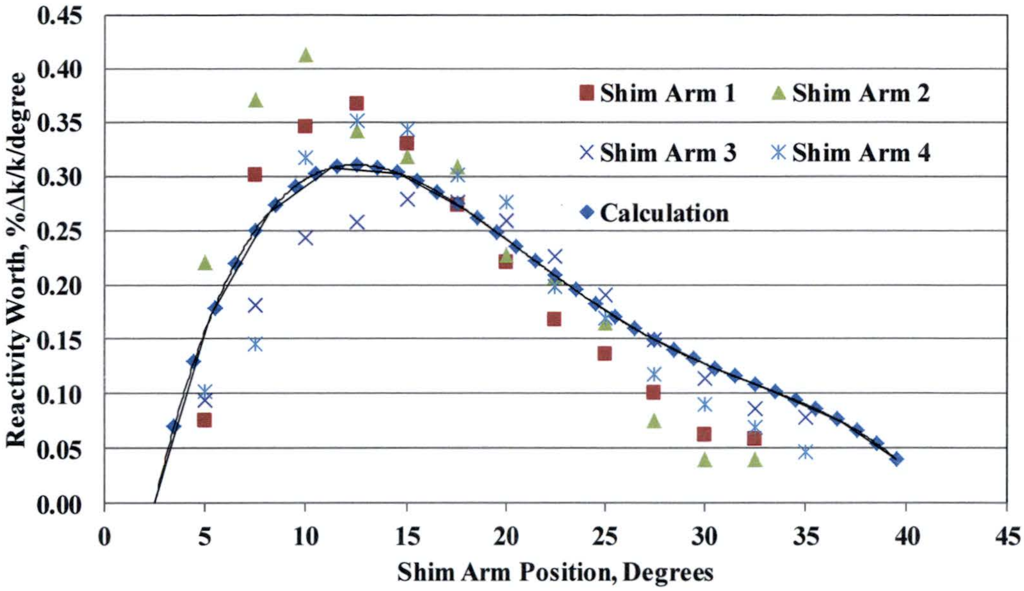

Figure 1-2 Differential shim arm worth as a function of position

RAI No. 2:

NUREG-1537, Part 1, Section 4.5.1, "Normal Operating Conditions," asks that "the applicant present information on the core geometry and configurations."

PSAR Section 4.5.1.2 states that 60 unique homogenized fuel element compositions are used to track the burnup of the 1020 fuel plates in the active core. The modelling approach reviewed indicates that there are no burnup gradients established in the fuel depletion calculations along the width of a plate, along the length of a plate, or from the plate-to-plate transition; the burnups are averaged over the upper and the lower plate of each assembly. Explain how your methodology ensures that the core thermal power and neutron flux spatial distributions are established so that reactivity predictions are suitably accurate and thermal-hydraulic (T-H) conditions are suitably conservative.

Response to RAI No. 2:

The current MCNP model using 60 different fuel element compositions is a doubling of the number of compositions relative to what was used in the previous submission to the NRC for license renewal and as computational tools improve and resources are available, more compositions will be used in the future. The ability to accurately predict reactivity with the current model is addressed in the response to RAI No. 1. The ability to provide conservative power distributions to assess thermal-hydraulic conditions is discussed in Section 4.6.1.2 of the PSAR:

"The power distribution in the fission plates is assumed to be given by the fission density as calculated by the computer code MCNPX. This is a conservative assumption, as 14% of the energy is in the form of γ-rays and neutrons, and will be deposited much more uniformly throughout the core. A conservative estimate of the energy deposited in the fuel is 95% (Hanson, 2005b). Another conservatism is the fact that burnup is assumed to be uniform over each half-element. In reality the distribution of burnup in a half-element is roughly proportional to power density and this tends to lower high power densities. This does not apply to fresh fuel but, as will be discussed below, the highest powers are in burned fuel elements. The degree of conservatism that is the result of not taking into account the burnup distribution is discussed in (Brown, 2013)."

As requested in RAI No. 12, a copy of (Brown, 2013) is included in a supplemental folder.

RAI No. 3:

The guidance in NUREG-1537, Part 1, Section 4.6, "Thermal-Hydraulic Design," states, in part, that "The calculational methodology should be applicable to the thermal-hydraulic operating conditions, and the applicant should justify its use."

a) The PSAR Section 4.6.2.1 states that the Sudo-Kaminaga critical heat flux (CHF) correlation was used to characterize the departure from nuclear boiling ratio (DNBR) of the NBSR. That discussion describes the CHF experiments conducted in that research project, but does not refer to or demonstrate the acceptability of the results obtained. Provide the basis for the acceptability of this correlation for the NBSR.

b) The PSAR Section 4.6.2.2 states that the Saha-Zuber criteria was used to estimate the onset of net vapor generation and that this condition is assumed to be indicative of the onset of flow instability. Provide the basis for the acceptability of this correlation for the NBSR.

Response to RAI No. 3a:

The Sudo-Kaminaga critical heat flux (CHF) correlation was developed specifically for vertical rectangular channels heated from both sides in nuclear research reactors [(Sudo, 1993) in Chapter 13 of the PSAR]. The correlation actually consists of four CHF equations (branches) and one of them is used to evaluate CHF depending on flow conditions (high-flow, intermediate up-flow, intermediate down-flow, and low-flow). It is noted that the low-flow CHF is correlated by using the flooding condition (counter-current flow limitation (CCFL)) at the upper end of the flow channel. The range of the experimental data used to develop the Sudo-Kaminaga CHF correlation is described in Section 4.6.2.1 of the PSAR and is reproduced in Table 3-1 below. The table also shows normal operating and startup accident conditions for the NBSR. The startup reactivity insertion accident with LEU fuel at the end-of-cycle (EOC) is considered because it shows the lowest minimum DNBR (2.01 at 16.1 s) for reactivity accidents. As shown in the table, the geometry and operating conditions (normal and accident) for the NBSR are all within the range of the experimental database for the Sudo-Kaminaga CHF correlation.

Table 3-1 Ranges for Sudo-Kaminaga correlation and NBSR operating and accident conditions

Parameter	Experiment	NBSR	
		Normal Operating	Startup Accident
Flow channel geometry	Vertical rectangular	Vertical rectangular	Vertical rectangular
Pressure (MPa)	0.1 to 4	0.1	0.1
Mass flux (kg/m^2-s)	-25,800 to 6,250	4,940 in the hot channel	4,980 in the hot channel[1]
Inlet subcooling (K)	1 to 213	72.8 at the inlet of hot channel	87.5 at the hot channel[1]
Outlet subcooling (K)	0 to 74	60.8 at the outlet of hot channel	69.5 at the outlet of hot channel[1]
Outlet quality	0 to 1.0	0	0
Heated length/equivalent hydraulic diameter, L/D_e	8 to 240	53.2	53.2
[1]At the time of the minimum DNBR			

In a later publication Kaminaga et al. [(Kaminaga, 1998) in Chapter 4 of the PSAR] refined the CHF correlation by performing experiments to investigate the effect of coolant subcooling when the flow is low. Based on the experimental results they modified the low-flow CHF equation (branch) with a correction factor that accounts for the beneficial effect of coolant subcooling. Table 3-2 shows the low-flow experimental conditions and the parameter ranges for the NBSR. The accident with throttling of coolant flow to the outer plenum is considered because the mass flux in the outer core becomes very small as the control valve DWV-1 closes. The ranges shown in Table 3-2 are applicable only to the modified low-flow equation. As the comparison shows in Table 3-2, two parameters (axial power peaking factor and L/D_e) are slightly outside the range of the experiments.

In their 1998 paper Kaminaga et al. did not observe any impact on the low-flow CHF due to the effects of axial heat flux distribution and peaking factor. The scatter in the test data about the low-flow CHF correlation did not exhibit any trend or pattern as a result of varying the axial peaking from 1.0 (uniform heat flux) to 1.6. It is thus reasonable to expect that the same non-dependence on peaking factor will hold when the axial peaking factor is extrapolated to 1.76, slightly beyond the upper range of the test condition. In developing the low-flow CHF correlation Kaminaga et al. used the maximum local heat flux to denote the wall heat flux when a CHF condition is detected in the test. The parameter L/D_e is thus irrelevant to the prediction of the CHF because the low-flow CHF correlation has no dependency on the actual axial location when the CHF condition is reached. Furthermore, as noted earlier, the low-flow CHF is correlated by using the flooding condition and the characteristic geometric parameter for CCFL is typically the hydraulic diameter D_e and not the L/D_e.

(Sudo, 1993) and (Kaminaga, 1998) are provided along with other supplemental material in a separate folder (see RAI No. 15).

Table 3-2 Ranges of modified equation of Sudo-Kaminaga correlation and NBSR operating and accident conditions

Parameter	Experiment	NBSR Loss-of-Flow accident[1]
Flow channel geometry	Vertical rectangular	Vertical rectangular
Pressure (MPa)	~ 0.1	0.1
Mass flux (kg/m^2-s)	0 to 73	27[2]
Inlet subcooling (K)	0 to 78	68.4[2] at the inlet of hot channel
Channel gap size (mm)	2.25 to 5	2.7[3]
Axial power peaking factor	1.0 to 1.6	1.31 ~ 1.76[4]
Equivalent hydraulic diameter, D_e (mm)	4.3 to 9.1	5.3
Heated length/equivalent hydraulic diameter, L/D_e	71 to 174	53.2

[1]Throttling of coolant flow to the outer plenum
[2]The flow conditions after the accident with LEU fuel at startup (SU) is examined because the minimum DNBR occurs in this case.
[3]The channel gap size of 2.7 mm is the smallest possible gap size and is assumed for the hot channel.
[4]The power peaking factor of 1.76 occurs in an upper plate of an LEU fuel element at SU. The highest power peaking factor with HEU fuel is 1.66 at SU.

Response to RAI No. 3b:

The first paragraph of Section 4.6.2.2 of the PSAR states:

"The most relevant instability for the NBSR, the Ledinegg static instability, has its origin in a simple effect. As water flow in a heated channel is reduced, a point will be reached where boiling will occur. At a later point significant amounts of vapor will be present in the channel. The presence of this vapor will increase the pressure drop, and when this effect is large enough, this increase will overwhelm the decrease in pressure drop arising from the flow decrease. This is known as the onset of flow instability. At this point, the overall pressure drop in the hot channel of a fuel element will increase, and flow will be reduced (if the channel spans an inlet and outlet header, with other, lower power channels in parallel). This condition causes a flow instability, which will result in rapid loss of adequate cooling for that channel".

Using similarity parameters (Nusselt number, Stanton number, and Peclet number), Saha and Zuber developed criteria to predict local conditions for net vapor generation in subcooled boiling

[(Saha, 1974) in Chapter 13 of the PSAR]. They examined available experimental data and plotted them on a Stanton number (St) and Peclet number (Pe) co-ordinate system as shown in the figure below. They defined Nusselt number (Nu) as $Nu = \frac{\dot{q}'' D_h}{k_f \Delta T_\lambda}$. The product of Pe and St is Nu. As shown in the figure below, there are two distinct regions and they determined that when $Pe \leq 70{,}000$, the criterion for net vapor generation is $Nu = 455$ and it is $St = 0.0065$ when $Pe > 70{,}000$.

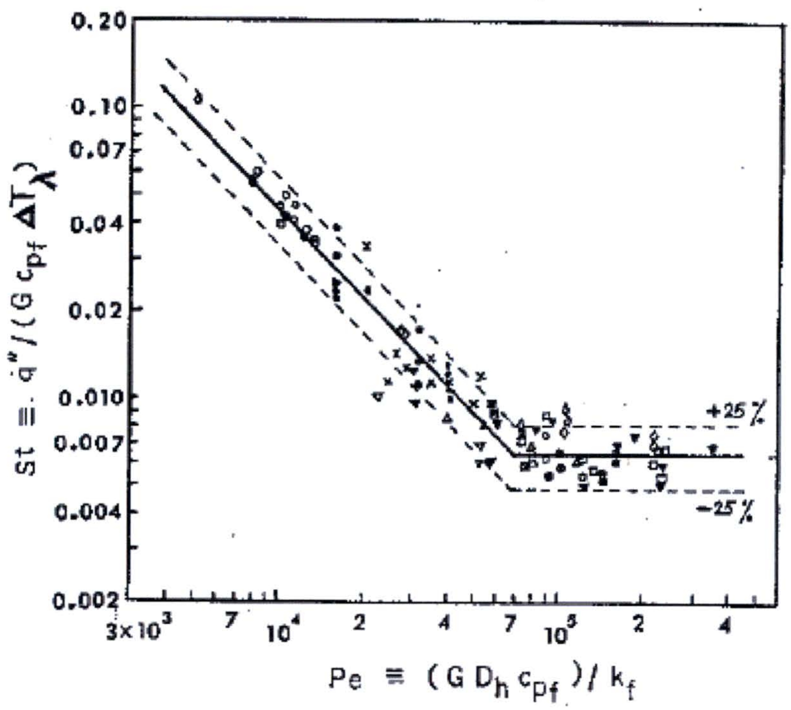

Fig. 2. PECLET NUMBER VS STANTON NUMBER AT THE POINT OF NET VAPOR GENERATION.

It should be noted that the Saha-Zuber criteria are a correlation to predict net vapor generation in subcooled boiling while flow instability (the Ledinegg static instability) occurs when a large enough amount of vapor exists in a flow channel. Therefore, the Saha-Zuber criteria are used in the analysis with the assumption that the onset of net vapor generation is a conservative threshold for onset of flow instability.

(Saha, 1974) is provided along with other supplemental material in a separate folder (see RAI No. 15).

RAI No. 4:

The guidance in NUREG-1537, Part 1, Section 13.1.3, "Loss of Coolant," states, in part, that "Some initiators of LOCAs [loss-of-coolant accidents] are the following: . . . failure or malfunction of some component in the primary coolant loop."

The PSAR, at various times, hypothesizes the failure of the DWV-19 valve (PSAR Section 13.3, 13.3.1, 13.5.5, etc.) as part of the LOCA/loss-of-flow accident (LOFA). However, Figure 13.1 in the PSAR illustrates no such valve in the NBSR system. Confirm whether valve DWV-19 is the correct nomenclature for the valve in question, or whether Figure 13.1 under review needs to be updated.

Response to RAI No. 4:

It is mentioned in Section 13.3 of the PSAR that the control valve DWV-19 is located upstream of the primary coolant pumps, but DWV-19 is not shown in Figure 13.1. Figure 13.1 should be replaced with a new schematic diagram of the NBSR primary system shown below (Figure 4-1). The new figure clearly shows that the control valve DWV-19 is located between the primary pumps (DP-1 through DP-4) and the reactor vessel outlet.

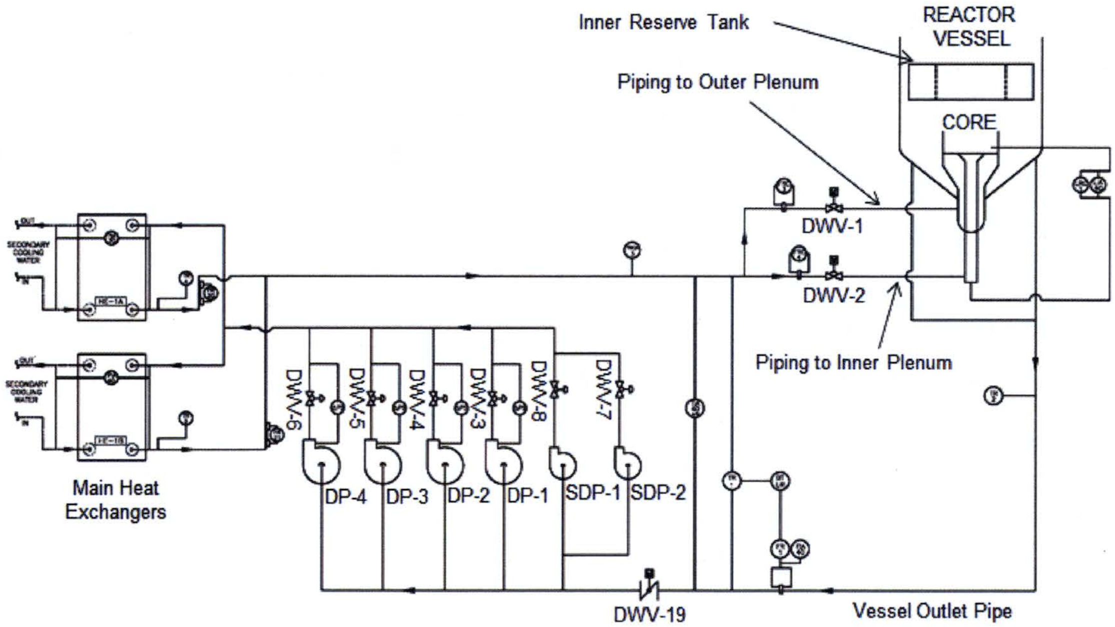

Figure 4-1 NBSR Primary System (will be new Figure 13.1 of PSAR)

RAI No. 5:

NUREG-1537, Part 1, Section 4.6, "Thermal-Hydraulic Design," states, in part, that "for the core geometry and the coolant thermal-hydraulic characteristics, a discussion to establish the fuel heat removal conditions that ensure fuel integrity such as fuel surface saturation temperature, . . ., departure from nucleate boiling and/or flow instability."

Figure 13.4 in the PSAR indicates that the model defined to describe for the T-H conditions - which has a distinct fuel meat and cladding in the heat structure - is different from the model used in the neutronics analysis, in which the meat and cladding appears to be homogenized. Confirm that the manner in which the power distribution is determined and translated into the T-H model is suitably conservative for DNBR analysis.

Response to RAI No. 5

As stated in Section 4.5.1.1 of the PSAR, the neutronics model explicitly represents "all 1020 fuel plates with explicit cladding." Figure 5-1, below, is a cross section of the fuel element model (on the left), showing the detail used for the fuel plates in each of the 30 fuel elements in the core model. It shows the 17 fuel plates with fuel meat and cladding (with the Zr interlayer homogenized with the cladding for the LEU fuel) represented explicitly as seen in the detail on the right (drawn on a different scale). It also shows the 18 coolant channels (albeit with mesh lines through their center), the two side plates (at top and bottom) and two outside plates.

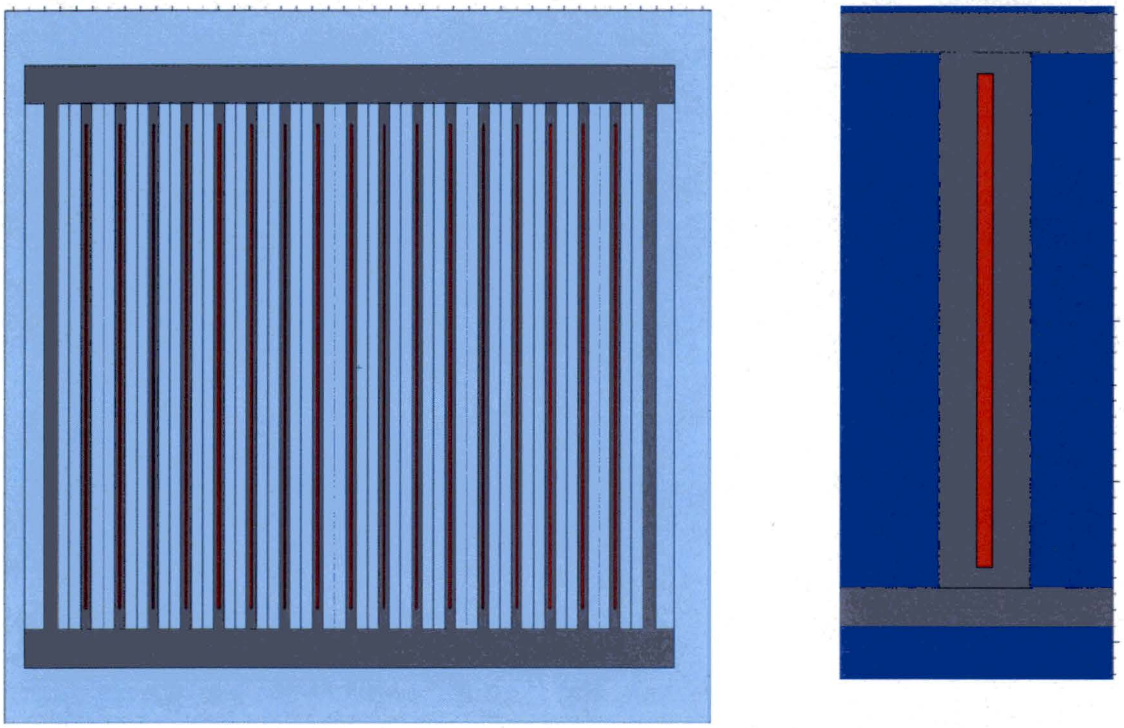

Figure 5-1 MCNPX modeling of fuel element cross section with detail of fuel plate

To obtain the power distributions used in the thermal-hydraulic model, each of the (30x34) 1020 fuel plates is divided into 14 axial meshes and three transverse meshes (approximately a 2x2 cm mesh). As explained in the response to RAI No. 2, the power distribution will be conservatively high. The use of the 14x3 mesh to capture the power distribution for use in thermal-hydraulic analysis is discussed in Section 4.5.3.2:

"The choice of mesh size for the MCNPX calculations is based on the observation that heat conduction in a fuel plate will result in a lateral heat flux profile (i.e. across the width of a fuel plate) that is flatter than the profile of the energy deposition due to fission, primarily due to the effect of conduction to the Al alloy at the ends of the plate. The lateral heat conduction problem was analyzed both analytically (Rowe, 2008) and numerically (Cheng, 2010). The results show that the average energy deposition per unit surface area of a mesh cell for a 2x2 cm mesh conservatively captures the maximum wall heat flux determined by solving the detailed heat conduction problem for a fuel plate. The acceptable mesh translates into three mesh intervals in the lateral direction and 14 mesh intervals in the axial direction for each fuel plate."

RAI No. 6:

NUREG-1537, Part 1, Section 4.5.2, "Reactor Core Physics Parameters," states, in part, that the applicant should provide the information on "the axial and radial distributions of neutron flux densities, justifications for the methods used, and comparisons with applicable measurements."

PSAR Section 13.2.2 states that the power distributions used are conservative. However, because the upper fuel plates were modeled as homogeneous within each assembly and the same was done for the lower plates, the resulting burnup distribution appears to be flat and may not represent accurately the power distribution that is appropriate for estimated critical position (ECP) calculations, DNBR, or accident analysis. Confirm that the manner in which the fuel material is described in the MCNP model leads to suitably accurate ECPs and is also used in a conservative manner for DNBR and accident analysis, or describe how additional factors or penalties are used to achieve acceptable results.

Response to RAI No. 6:

The fact that the MCNP model leads to suitably accurate ECPs and is also used in a conservative manner for DNBR and accident analysis is explained in the responses to RAIs No. 2 and 5.

RAI No. 7:

NUREG-1537, Part 1, Section 4.6, "Thermal-Hydraulic Design," states, in part, that "The calculational methodology should be applicable to the thermal-hydraulic operating conditions, and the applicant should justify its use."

The NBSR RELAP model combines the coolant loops into a single flow path. It is not clear that such a model can model multi-loop effects conservatively (e.g., single pump failure, single shaft seizure, LOCA, LOFA, and the asymmetric effects that they have on reactor performance under accident conditions [e.g., throttling flow to outer plenum] etc.). If there are additional components in the model, and the actual reactor, that contribute to this understanding (e.g., check valves), then provide an updated graphic that shows such components.

To assist in the staff assessment of the RELAP model used for such purposes, provide the ASCII text input file of the actual DNBR model used. We may also need to obtain access to the NBSR drawings to verify certain aspects of the model.

Response to RAI No. 7:

Only components (primary pumps, shutdown pumps, and heat exchangers) are combined into one effective component and loops are not lumped together in the RELAP5 model. Figure 4-1 (above) shows a schematic diagram of the NBSR primary system. This figure includes the important components and flow paths that are considered in the RELAP5 input model, as well as some gauges measuring pressure, temperature, differential pressure, mass flow, etc. The figure shows that the four primary coolant pumps (DP-1 through DP-4) operate in parallel. The pipe downstream of the DWV-19 branches off into four separate pump suction lines and the four discharge lines of the pumps are all connected to one pipe. The pipeline downstream of the heat exchangers is split into two flow paths, one to the inner plenum and the other to the outer plenum.

Figure 1.1 of the PSAR shows the NBSR vessel internals and rector core. Labels 7 and 8 represent the outer and inner plena, respectively, and there are 24 and 6 fuel elements located in the outer and inner cores. Figure 4-1 shows these outer and inner cores connected with the "piping to outer plenum" and "piping to inner plenum," respectively. Figure 4-1 also shows two shutdown pumps (SDP-01 and SDP-02), two heat exchangers, and the control valves (DWV-1, DWV-2, and DWV-19) isolating the reactor vessel.

Figure 7-1 (Figure 13.2 of PSAR) shows the nodal diagram of the primary system of the NBSR. As shown in the figure, most of the coolant loops are modeled separately, including the "piping to outer plenum" and "piping to inner plenum." The flow channels in the core are modeled in detail enough to appropriately simulate the hot cells, hot plates, and average plates in the inner and outer cores as shown in Figure 7-1.

In the accident assuming seizure of a single pump, coolant flow through the damaged pump will decrease significantly or stop. The control valves (DWV-3 through DWV-6 in Figure 4-1) at the discharge lines of the primary coolant pumps are pneumatic valves. If the coolant flow rate becomes small enough at the discharge line of one primary pump, the control valve at that discharge line will close due to a low ΔP signal. This configuration prevents any backflow, to the pump coasting-down, from occurring.

The other three important loss-of-flow accidents (LOFAs) are throttling of coolant flow to the inner and outer plena due to closure of DWV-2 and DWV-1 (see Figure 4-1) and a loss of primary flow caused by closure of DWV-19 (see Figure 4-1). These accidents are simulated by closing VALVE-50, VALVE-51, and VALVE-26 (see Figure 7-1). Since the control valve DWV-19 is not explicitly modeled, the accident of closure of DWV-19 is modeled by closing the valve at the primary pump outlet (VALVE-26). The valves (DWVs-7 and 8 in Figure 4-1 and VALVE-83 in Figure 7-1) at the discharge lines of the shutdown pumps are closed in the LOFA analysis. The control valves are assumed to close in a way to make the coolant flowrate smaller in the analysis. Since the closure of each control valve along with its associated flow path is modeled separately, the LOFAs are simulated appropriately without skewing the coolant flow behavior in the primary system of the NBSR.

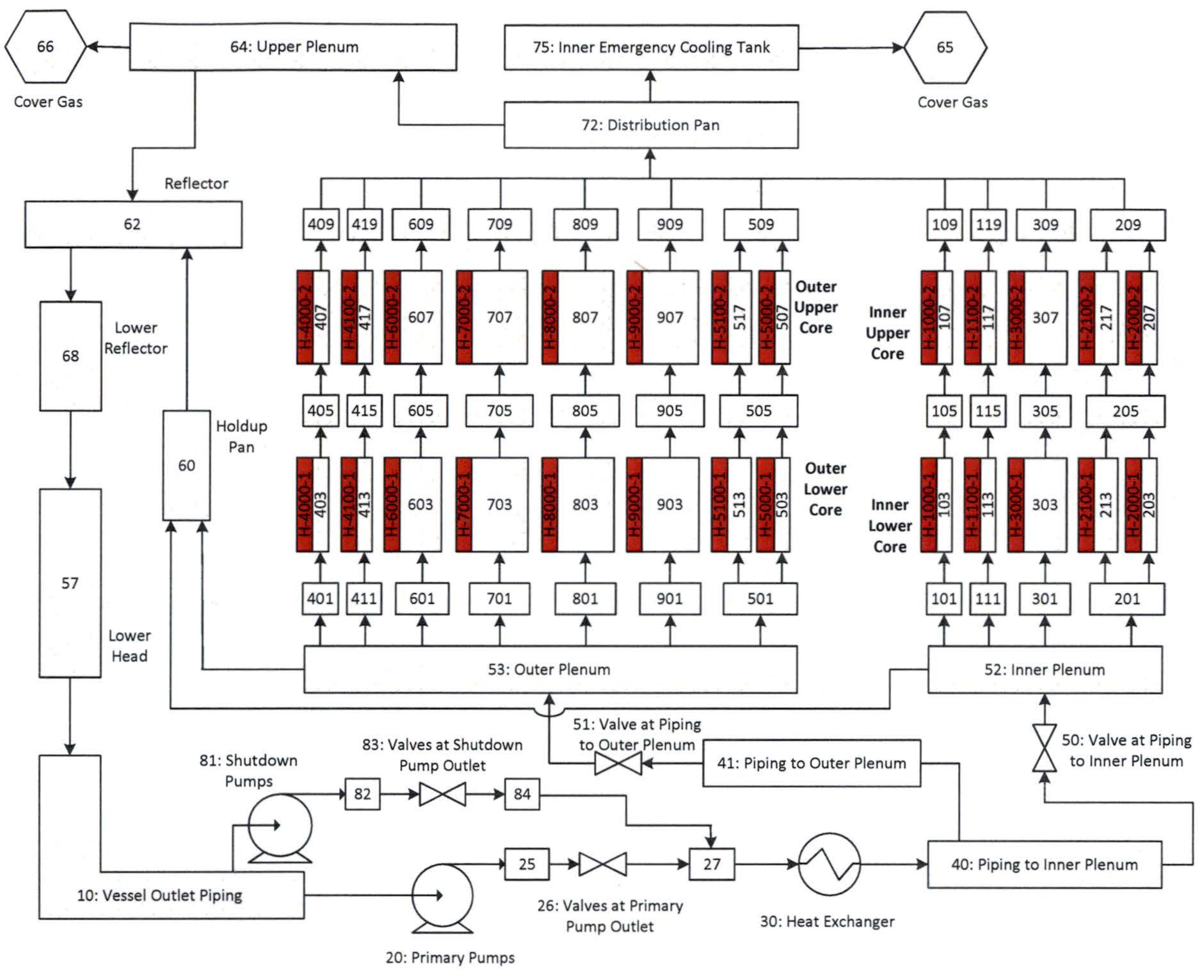

Figure 7-1 RELAP5 nodal diagram for NBSR primary system

Figure 7-2 (Figure 13.7 in the PSAR) shows the nodal diagram of the NBSR primary system that is used to analyze loss-of-coolant accidents (LOCAs). (The model shown in Figure 7-1 is used to simulate all accidents except for LOCAs.) It is expected that the NBSR core is led to the most severe conditions when a pipe break occurs between the outer plenum and DWV-1, the inner plenum and DWV-2, or the vessel outlet and DWV-19 (see Figure 4-1) because the reactor vessel cannot be isolated and the coolant continues draining from the vessel and/or the fuel elements. These accidents are simulated by opening VALVEs-1 and 2 and closing VALVE-51 for the guillotine break LOCA (GBLOCA) at the piping to the outer plenum, by opening VALVEs-23 and 32 and closing VALVE-70 for the GBLOCA at the piping to the inner plenum, and by opening VALVEs-3 and 22 and closing VALVE-102 for the GBLOCA at the vessel outlet piping (see Figure 7-3). Small break LOCAs are modeled by opening VALVE-12 or VALVE-33 and the valve opening (flow) area is determined by the break size. Small break at the vessel outlet piping is not simulated because the flow channels are always filled with coolant, which means that there is adequate cooling for the fuel plates. The significant LOCAs are simulated at the appropriate locations in the NBSR piping system. Therefore, there is no skew of the coolant flow behavior in the primary system in the predictions when the NBSR LOCAs are analyzed.

Based on the discussions given above, it can be concluded that the non-LOCA and LOCA models of the NBSR are detailed enough to simulate all possible postulated accidents conservatively or nearly realistically.

The MED file (the SNAP version) of the RELAP5 steady-state input model with LEU fuel at SU is provided in a separate folder. This was the file that had been determined by NRC to best satisfy the request in this RAI. Versions of RELAP5 and the SNAP used in the analysis are 3.3hj and 2.4.1, respectively.

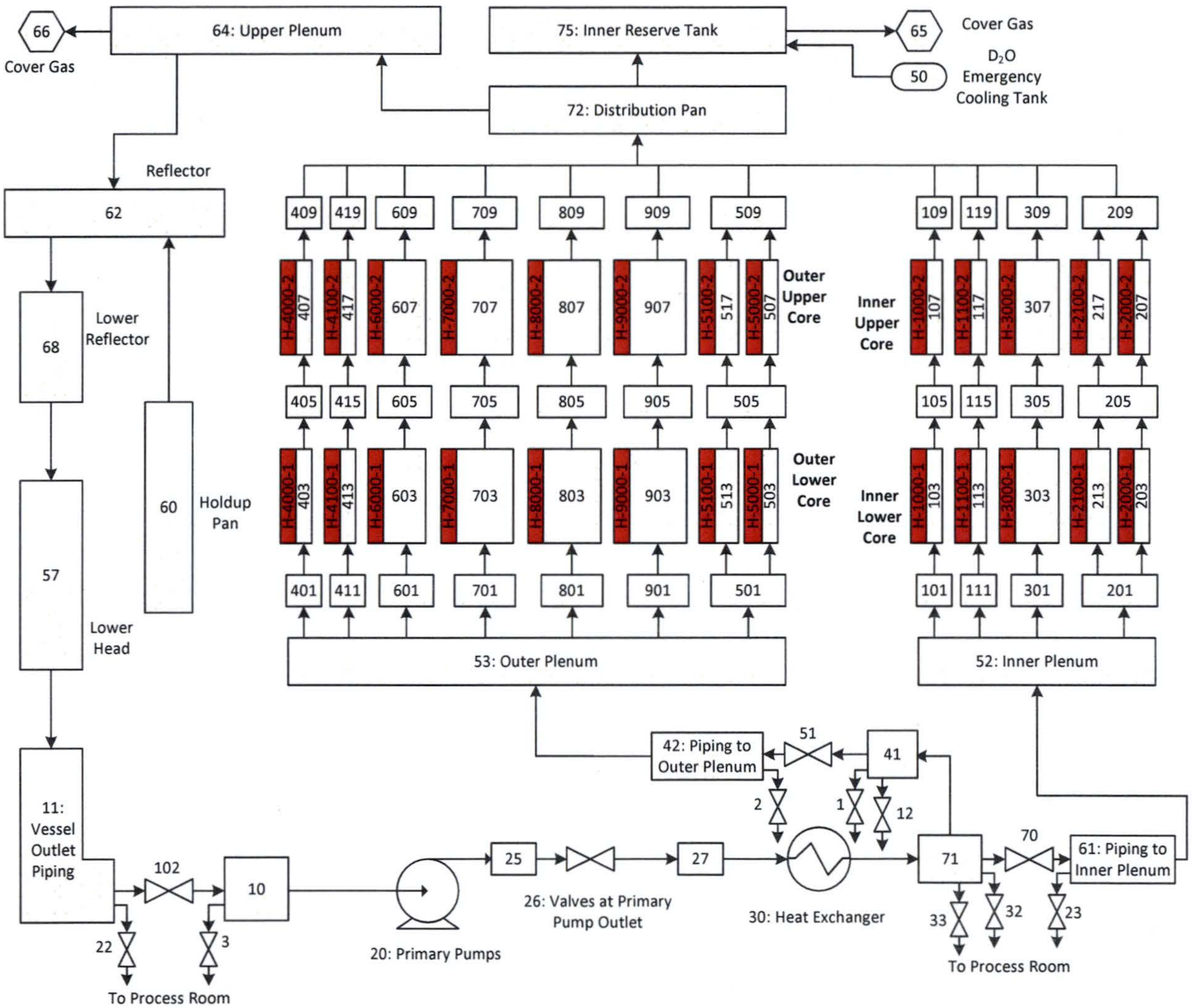

Figure 7-2 TRACE nodal diagram for NBSR primary system for LOCA analysis

RAI No. 8:

NUREG-1537, Part 1, Section 13.1.2, "Insertion of Excess Reactivity," asks for the analysis of insertion of excess reactivity that includes a ramp insertion of reactivity by drive-initiated motion of the most reactive control rod or shim rod, or ganged rods, if possible. PSAR Section 13.4.2.1 describes an operator induced rod withdrawal error. It is unclear if this analysis meets the intent of the guidance. Identify the maximum blade withdrawal rate and the worth of the maximum worth blade, including any applicable uncertainties and ensure that the supplied analysis models this accident in a suitably conservative manner.

Response to RAI No. 8

The analysis of the so-called "startup accident" assumes a conservative reactivity insertion rate equal to the Technical Specification (TS) limit of 0.05 %Δk/k/s (TS 3.2.1). This rate is greater than is possible with any or all of the shim arms or with the regulating rod (see discussion below).

Shim arm reactivity worth is shown in Figure 1-2 (in the response to RAI No. 1). The shim arms can only move at the fixed rate of 0.045 degree/s and hence, the maximum shim arm reactivity insertion rate (which is only relevant near or above criticality when the shim arms are near the center regions of their movement) is less than that assumed in the accident analysis. The regulating rod has a constant differential worth as can be seen in Figure 4.15 in the PSAR. Again the withdrawal rate is fixed; it takes 15.5 seconds to withdraw the rod. The total worth in Figure 4.15 is 0.65 %Δk/k and hence the maximum reactivity insertion rate based on using the regulating rod is 0.042 %Δk/k/s.

Additional conservative assumptions used in the analysis are that reactor trip occurs at 130% of full power rather than the actual setting of 125%; the calculation does not consider any fuel or moderator temperature feedback; and does not consider the period scram available even though it is operable below 2 MW.

RAI No. 9:

The guidance in NUREG-1537, Part 1, Section 13.1.4, "Loss of Coolant Flow," asks for the analysis of loss of coolant flow accident. PSAR Section 13.5.2.1 included the sequence of events (SOE) for the seizure of one primary pump. It is unclear whether this SOE is conservatively modeled, given the fact that the behavior of an idle loop, including backflow, cannot be modeled using the RELAP model described. Provide a justification for the SOE specified using the supplied RELAP model, and show that the resulting analysis is justified and suitably conservative.

Response to RAI No. 9:

The accident with seizure of a single pump is simulated appropriately and conservatively without skewing the coolant flow behavior in the primary system because the flow paths are modeled as closely as possible to the real loop configuration and the pump behavior is modeled conservatively. Refer to the response to RAI No. 7 for a discussion about not having back flow to a damaged pump.

In the accident scenario with seizure of a single pump (the results of a single pump failure accident are bounded by the consequences assuming seizure of a single pump), coolant flow through the primary loop will decrease over a finite time interval until about one-third flow reduction is achieved. Since the RELAP5 model lumps all three pumps (only three out of the four pumps are running during normal operation) into one effective pump (PUMP-20 in Figure 7-1), the seizure of one of the pumps is modeled by an instantaneous step reduction (without coasting-down) in the pump speed to two-thirds of full speed. This is conservative not only because it assumes an immediate decrease of pump flow but also due to the fact that the flowrate with only two pumps operating would actually be higher than two-thirds of full flowrate. This is confirmed by the characteristic curves for the main coolant pumps of the NBSR shown in Figure 9-1 [(NIST, 2010a) in Chapter 13 of the PSAR]. The figure shows flowrates of 7,000 gpm with two pumps and about 9,000 gpm with three pumps. With less coolant flow, the core will be in a more severe (conservative) condition in terms of removing heat from the fuel plates.

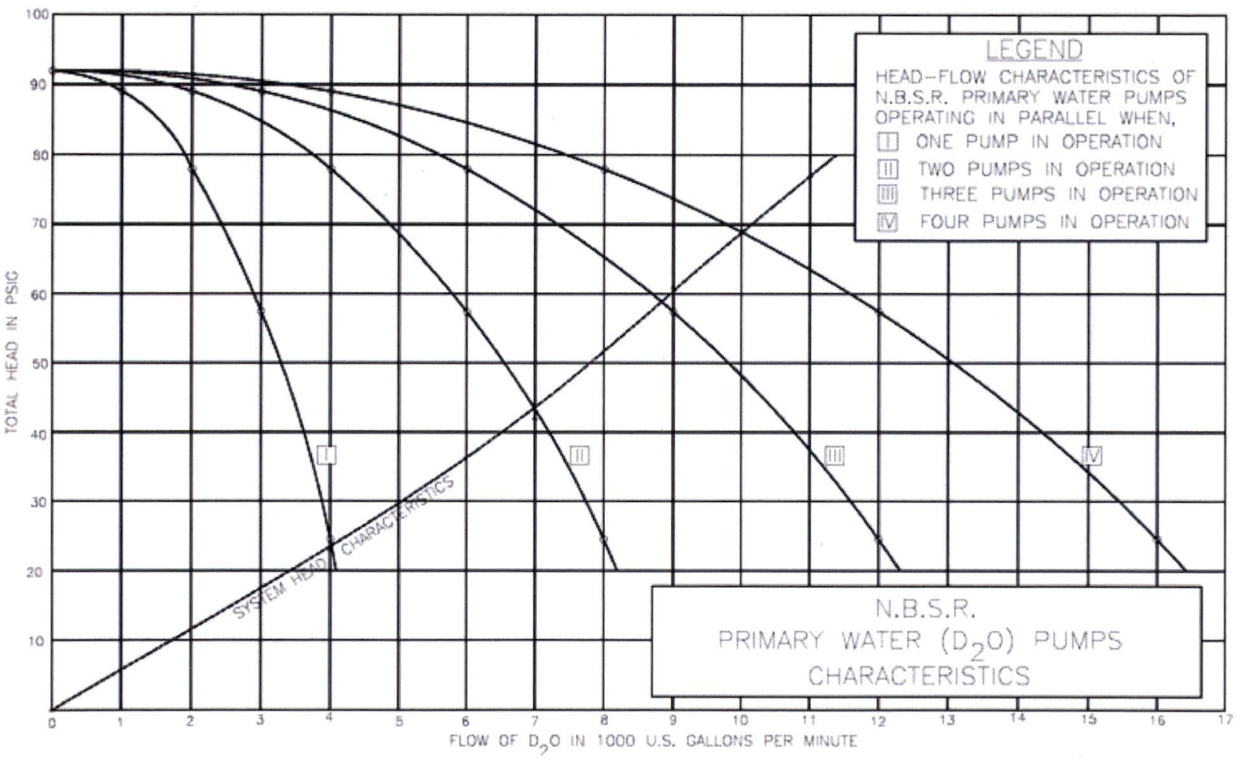

Figure 9-1 Main Coolant Pump Characteristics

RAI No. 10:

NUREG-1537, Part 1, Section 13.1.4, “Loss of Coolant Flow,” asks for the analysis of a loss of coolant flow accident. PSAR Sections 13.5.3.1 and 13.5.4.1 discuss the SOE for throttling coolant flow to the outer/inner plenum. It is unclear whether this SOE is conservatively modeled, given the fact that the behavior of an idle loop cannot be modeled using the RELAP model described. Provide a justification for the SOE specified using the supplied RELAP model and show that the resulting analysis is justified and suitably conservative. Describe in details the location of piping and valves so as to understand whether there is any significant potential for asymmetric flow.

Response to RAI No. 10:

The accident scenarios with throttling of coolant flow to the inner and outer plena are simulated appropriately and conservatively without skewing the coolant flow behavior in the primary system because the flow paths are modeled as closely as possible to the real loop configuration and the control valves are closing in a manner to make the coolant flow smaller in the analysis. Refer to the response to RAI No. 7 for detailed discussion.

RAI No. 11:

NUREG-1537, Part 1, Section 13.1.1, "Maximum Hypothetical Accident," asks for the analysis of maximum hypothetical accident (MHA).

- Since NBSR is a closed system that contains the fission products, there is virtually no dose to occupational workers or public from an in-reactor failed fuel assembly, which is the MHA analyzed. However, the NBSR technical specifications (TSs) mention fueled experiments. Consider a failed experiment, a failed fueled experiment, a fuel handling accident, and a fuel disassembly accident occurring under conditions and at various locations (e.g., spent fuel storage locations, hot cells, fume hoods, reactor bay, etc.) that maximize their potential impact, and then determine whether one of these events, or the existing failed fuel assembly accident is the MHA for NBSR. Analyze the impact of the maximum source term in terms of the resulting dose to occupational workers and the public. Provide assumptions and analysis for these events for staff review.

- For the fuel disassembly accident, consider events such as debris impingement, cladding longitudinal tears, cutting blade fracture, or any other credible failure that could lead to breaching the cladding-fuel interface.

- The PSAR Table 13.21 indicated that there are smaller HEU inventories than those in the 2004 SAR. Explain the differences and explain the nomenclature used.

- Confirm which HOTSPOT version was used in the licensee analysis. Provide HOTSPOT output for the limiting case.

- Explain why the filters cited on page 148 are not controlled by the TSs.

- Address the following possible inconsistencies:
  Should the reference to Table 13.24 be to 13.21 on page 146?
  Should the reference to Table 13.25 be to 13.22 on page 147?
  Should the reference to Table 13.26 be to 13.23 on page 148?
  Should the reference to Table 13.27 be to 13.24 on page 148?

Response to RAI No. 11: (Each bullet item above is repeated in italics below)

- *Since NBSR is a closed system that contains the fission products, there is virtually no dose to occupational workers or public from an in-reactor failed fuel assembly, which is* *the MHA analyzed. However, the NBSR technical specifications (TSs) mention fueled experiments. Consider a failed experiment, a failed fueled experiment, a fuel handling accident, and a fuel disassembly accident occurring under conditions and at various locations (e.g., spent fuel storage locations, hot cells, fume hoods, reactor bay, etc.) that maximize their potential impact, and then determine whether one of these events, or the existing failed fuel assembly accident is the MHA for NBSR. Analyze the impact of the maximum source term in terms of the resulting dose to occupational workers and the public. Provide assumptions and analysis for these events for staff review.*

The MHA considered in the PSAR has always been accepted as the maximum hypothetical accident taking into account all other hypothetical accidents, including those mentioned in this RAI. This is explained here, in answer to the next bullet item and in the responses to RAIs 12, 13, and 14.

Although there is mention of fueled experiments in the TSs, there never has been, and there are no plans for, any fueled experiments, as that is not part of the mission of the NCNR. The amount of radioactivity involved in a particular experiment (which is independent of whether the fuel is HEU or LEU) is controlled by TSs 3.8.2 and 6.5, which require a thorough hazards review before an experiment can be initiated. These experiments have been analyzed for previous SARs. The only large sources of radioactivity are the fuel elements within the core and when removed from the reactor vessel. Several hypothetical accidents with fuel are considered.

The spent fuel can only be handled in a controlled fashion. TS 3.9.2.2 prohibits the movement of a fuel element out of the reactor vessel "unless the reactor has been shut down for a period equal to or longer than one hour for each megawatt of operating power level." This is to ensure that a fuel element will not melt even if exposed to air. Based on measurements, the temperature of the hottest element would remain less than 416°C without auxiliary coolant, that is, with just stagnant air[b]. This result is for HEU fuel and would have to be checked for the LEU core[c].

The results given in the PSAR for the MHA (Section 13.8) were obtained using conservative assumptions. They show that the dose to the public has a safety factor of more than (100/6) ~16 and for the NBSR staff it is either (5/0.3) ~16 or (5/2.1) ~2.4. Any release outside of the reactor vessel would still need to migrate to rooms where there was staff present and still go through the ventilation system before getting out of the confinement, adding further conservatism to the values.

---

[b] J.M. Rowe, "Maximum Temperature of Fuel Elements for the NBSR in Stagnant Air," memo to W. Richards, NIST Center for Neutron Research, February 16, 2007.

[c] The result is acceptable for HEU fuel because it is lower than the blister temperature (450°C) and the clad melting temperature (taken by NRC to be 530°C). However, if blister temperature is used as a criterion for LEU fuel (conservatively taken as 380°C), rather than clad melting temperature, TS 3.9.2.2 would need to be modified in the future to allow for a longer cooling period before removing any LEU fuel from the reactor vessel.

- *For the fuel disassembly accident, consider events such as debris impingement, cladding longitudinal tears, cutting blade fracture, or any other credible failure that could lead to breaching the cladding-fuel interface.*

The cutting of fuel elements before they can be taken away from the NBSR is done under controlled conditions that preclude the possibility of cutting into a fuel plate. Furthermore, the two side plates and two outside plates that provide the outside box of the fuel element, shield the fuel plates from damage that might be the result of something striking the element. Since a complete transverse cutting of the fueled section of a fuel element would result in fission product release from the region of the fuel plate near the cut, it is estimated that the release would be less than 1% of that predicted for the MHA, under the absolute worst conditions.

- *The PSAR Table 13.21 indicated that there are smaller HEU inventories than those in the 2004 SAR. Explain the differences and explain the nomenclature used.*

Table 13.21 in the PSAR (which should be identified as Table 13.22 on page 147) provides the activity of the key isotopes determined for a half-element whereas the data in the 2004 document is for a complete fuel element. In Table 11-1 below, the results from the PSAR are shown multiplied by two (as used for the MHA analysis) and compared with the older results. (The nuclides are identified in Table 11-1 as isomers with the usual nomenclature whereas in Table 13.21 an asterisk had been used to designate a footnote to explain that an isotope was an isomer.) They show that the newer results are *higher* than the older results for 17 of the 23 isotopes listed. The reason for the differences is that they were obtained using two very different methods.

Table 11-1 Activity of I, Kr, and Xe Isotopes in an HEU Fuel Element

Nuclide	2004 Document (Ci)	2014 Document (Ci)	Nuclide	2004 Document (Ci)	2014 Document (Ci)
I-130	9.36E+02	1.01E+02	Kr-85m	7.01E+03	8.58E+03
I-130m	3.29E+02	7.50E+01	Kr-87	1.42E+04	1.86E+04
I-131	1.59E+04	1.66E+04	Kr-88	2.00E+04	2.50E+04
I-132	2.41E+04	2.92E+04	Xe-131m	1.78E+02	4.54E+01
I-132m	-	6.84E+01	Xe-133	3.66E+04	3.64E+04
I-133	3.72E+04	4.72E+04	Xe-133m	1.10E+03	9.46E+02
I-133m	7.11E+02	3.08E+03	Xe-134m	-	3.58E+02
I-134	4.20E+04	5.60E+04	Xe-135	9.42E+02	3.64E+03
I-134m	2.41E+03	2.62E+03	Xe-135m	6.26E+03	8.34E+03
I-135	3.47E+04	4.50E+04	Xe-137	3.31E+04	4.36E+04
Kr-83m	2.94E+03	3.88E+03	Xe-138	3.44E+04	4.50E+04
Kr-85	7.91E+01	4.84E+01			

The older analysis was done using the ORIGEN2 code [(Croff, 1980) in Chapter 13 of the 2004 SAR] and assuming that the activity would be the result of burning a fuel element for eight cycles with an eleven day cooling period between cycles. The power in a fuel element was the core average (20MW/30 elements) during the irradiation period. The one-group cross sections used in the solution to the Bateman equations were from a library generated for a heavy water CANDU reactor; however, results are not very sensitive to the spectrum used to calculate the library.

The newer analysis used the CINDER'90 code.[d] The analysis is based on the MCNPX calculations (utilizing CINDER'90 for the burnup) done for the equilibrium core. The compositions in any half-element (each half-element has a unique composition) are obtained taking into account the history of that particular half-element, rather than by assuming an average power[e]. An element that has completed eight cycles has had its composition tracked in each of the specific locations that the half-element occupied in each cycle. A 63-group flux spectrum is generated by MCNPX and used with the CINDER'90 63-group library to generate the one-group data needed to solve the burnup equations. The composition of a limiting half-element is then used in a final stand-alone CINDER'90 calculation for five days to obtain the activity in Curies. This additional calculation circumvents a minor problem in the coupling of CINDER'90 and MCNPX that lumps the ground and isomer states together for some isotopes. The final calculation has the equilibrium distribution of isomer vs ground states; important because of the high activity of some of the isomers. This methodology is clearly more rigorous than the original ORIGEN2 analysis. Furthermore, CINDER'90 uses much newer nuclear data than ORIGEN2 used. The PSAR calculation uses a 38.5 day cycle and a 10.5 day cooling period; values more realistic than those used for the 2004 SAR.

- *Confirm which HOTSPOT version was used in the licensee analysis. Provide HOTSPOT output for the limiting case.*

HOTSPOT Version 2.07.1, dated 2010 was used for the calculations. A portion of output from the code for the MHA is found in a supplemental folder (see RAI No. 15).

- *Explain why the filters cited on page 148 are not controlled by the TSs.*

The filters referenced on page 148 are, in fact, required by TS 3.5 and are tested in accordance with TS 4.5(3)

- *Address the following possible inconsistencies:*
  Should the reference to Table 13.24 be to 13.21 on page 146?
  Should the reference to Table 13.25 be to 13.22 on page 147?
  Should the reference to Table 13.26 be to 13.23 on page 148?
  Should the reference to Table 13.27 be to 13.24 on page 148?

The tables became mislabeled after Table 13.21 on page 136. Table 11-2 below shows the corrections needed for the table captions as well as the references to the tables in the text. Table 11-2 covers the tables in the RAI and one additional table.

---

[d] The reference (Cowell, 2008) given in Chapter 13 of the PSAR is incorrect. The correct reference is W.B. Wilson, S.T. Cowell, T.R. England, A.C. Hayes, and P. Moller, "A Manual for CINDER'90 Version 07.4 Codes and Data," LA-UR-07-8412, Los Alamos National Laboratory, March 2008.

[e] Details of the burnup model are found in Section 4.5.1.2 of the PSAR.

Table 11-2 Corrections to table numbering in Chapter 13

Table No. in PSAR	Correct Table Number	Reference in PSAR	Correct Reference
Table 13.21 (p 147)	Table 13.22	Table 13.24 (p 146)	Table 13.22
Table 13.22	Table 13.23	Table 13.25 (p 147)	Table 13.23
Table 13.23	Table 13.24	Table 13.26 (p 148)	Table 13.24
Table 13.24	Table 13.25	Table 13.27 (p 148)	Table 13.25
Table 13.25	Table 13.26	Table 13.28 (p 149)	Table 13.26

RAI No. 12:

NUREG-1537, Part 1, Section 13.1.5, "Mishandling or Malfunction of Fuel," asks for the analysis of mishandling or malfunction of fuel. PSAR Section 13.9 is titled "Mishandling, malfunction, or misloading of fuel." However, only misloading is analyzed. Provide a comprehensive analysis of both mishandling and malfunction events, or provide a justification for why such analysis is not required.

Response to RAI No. 12:

The discussion of mishandling or malfunction of fuel in Section 13.9 refers to the analysis in [(NBS, 1980) referenced in Chapter 13 of the PSAR]. That analysis discusses the low probability of an initiating event and the ability to detect any radioactivity released. Nevertheless, the radiological consequences of some hypothetical accidents were analyzed.

Operational limits provide some of the protection and the top shielding plug of the reactor is never removed while there is fuel in the core; precluding the potential for a heavy object to fall on the core). Also, since an HEU fuel element only weighs ~25 lb (and only ~16 lb in water) and an LEU element ~28 lb, dropping of an element in water is only expected to result in dents to the external non-fueled portions of the element. Any malfunction of fuel is bounded by the MHA analysis.

Instrumentation is present to pick up the release of any radioactivity into either the primary circuit, the secondary, or during the movement of fuel to the spent fuel pool. This allows for mitigating and protective actions to be put in place.

The previous analysis also considered the consequences of hypothetical accidents with the release of fission products. The analysis of a heavy object dropping onto the fuel rack in the spent fuel pool was analyzed using the guidance in NRC Regulatory Guide (RG) 4.2.[f] The analysis of a fuel cask drop was analyzed using the guidance in NRC RG 4.1.[g] For both

[f] "Preparation of Environmental Reports for Nuclear Power Stations," Regulatory Guide 4.2, Version 2, U.S. Nuclear Regulatory Commission, July 1976.

[g] "Radiological Environmental Monitoring for Nuclear Power Plants," Regulatory Guide 4.1, Revision 2, June 2009.

incredible accidents the dose to the public was well within acceptable limits.

RAI No. 13:

NUREG-1537, Part 1, Section 13.1.6, "Experiment Malfunction," asks for the analysis of experimental malfunction. PSAR Section 13.10 describes experiment malfunction, but did not characterize dose coming from fueled experiments such as those allowed under the TSs 3.9.1(1) and the basis. Provide your comprehensive analysis of the experimental malfunction.

Response to RAI No. 13:

The response to this RAI is found in the response to the first bullet item in RAI No. 11.

RAI No. 14:

NUREG-1537, Part 1, Section 13.1.6, "Experiment Malfunction," asks for the analysis of experimental malfunction. Confirm whether there are hot cells, fume hoods, or glove boxes at NBSR connected to a ventilation system that can exhaust to public receptors.

Response to RAI No. 14:

The building stack is a split stack with one side handling all reactor ventilation and the other handling the radiological lab area ventilation. There are chemical fume hoods and a glove box connected to the reactor ventilation system that exhaust to public receptors. These are released and monitored through the reactor side of the stack. There are also other radiological laboratories with fume hoods and a glove box in the facility that are monitored and released through the lab side of the stack.

The NCNR does not have a hot cell facility.

RAI No. 15:

Provide reference copies of Brown 2013, as cited in PSAR 13.2.2, and NBS 1980, as cited on page 149.

Response to RAI No. 15:

The references requested are found in a separate folder with other files requested in RAI No. 7 and No. 11. The following is a list of all files associated with this response to RAIs.

- (Brown, 2013)
- (NBS, 1980)
- RELAP5 input deck
- HOTSPOT output
- (Sudo, 1993)
- (Kaminaga, 1998)
- (Saha, 1974)